A sensorless approach for tracking control problem of tubular linear synchronous motor

Nguyen Hong Quang[1], Nguyen Phung Quang[2], Nguyen Van Lanh[3]
[1]Faculty of Mechanical, Electrical, Electronics Technology, Thai Nguyen University of Technology, Thai Nguyen City, Vietnam
[2]Institute for Control Engineering and Automation, Hanoi University of Science and Technology, Hanoi, Vietnam
[3]School of Electrical and Data Engineering, Faculty of Engineering and Information Technology, University of Technology Sydney,
Sydney, Australia

ABSTRACT

As well-known, linear motors are widely applied to various industrial applications due to their abilities in providing directly straight movement without auxiliary mechanical transmissions. This paper addresses the sensorless control problem of tubular linear synchronous motors, which belong to a family of permanent magnet linear motor. To be specific, a novel velocity observer is proposed to deal with an unmeasurable velocity problem, and asymptotic convergence of the observer error is ensured. Unlike other studies on sensorless control methods for linear motors, our proposed observer is designed by regrading unknown disturbance load in the tracking control problem whereas considering theoretical demonstrations. By adjusting controller parameters properly, the position and velocity tracking error converge in arbitrary small values. Finally, the effectiveness of the proposed method is verified in two illustrative examples.

Corresponding Author:

Nguyen Hong Quang
Faculty of Mechanical, Electrical, Electronics Technology, Thai Nguyen University of Technology
666, 3/2 Street, Tich Luong Ward, Thai Nguyen City 251750, Vietnam
Email: quang.nguyenhong@tnut.edu.vn

1. INTRODUCTION

During the past few years, tubular linear synchronous motors (TLSM) have been intensively applied to various applications including robotics, transportation, and vehicle systems because of the absence of mechanical reduction and transmission devices (gears and lead screws) permits to obtain higher precision and reduced dimensions in comparison with rotary motors. Recently, the merits of using TLSM have been pointed out by [1]-[3], which can be listed as low cost, the durable structure, reliable operation. In addition, there has been a large number of researches devoted to applications of TLSM such as active vehicle suspension [4], the planar magnet array [5], jetting dispenser [6], and two-dimensional nanopositioning [7]. More recently, the progress of modern control engineering has been toward the tracking problem of TLSM, which can be noted as thrust optimization [8], model predictive control [9], [10], and fuzzy control [11], [12].

Tubular linear synchronous motors whose structure as shown in Figure 1 contains a tube (slider) with mounted drive magnets, and three phases winding in stator placed differently 120° of electrical angle. Without auxiliary reducer or transmission, TLSM is capable of operating effectively by eliminating mechanical hysteresis. That however also rises the sensitiveness on the movement of slider due to frictional force, load variation, and non-sinusoidal flux. These unexpected forces shrink performance of the motion system both the transver-

sal and in the longitudinal direction. In recent years, there has been a majority of works devoted to improving the position tracking the performance of linear motor systems under the impact of external disturbance [13]. Besides, a backstepping sliding mode controller based on nonlinear disturbance observers was created by [14], [15] aimed at obtaining tracking performance as well as disturbance rejection. An adaptive robust controller was proposed by [16], in which the dead-zone compensation technique is applied to guarantees tracking performance and system robust against uncertainties. Furthermore, the researchers in [17] present an effective neural network learning controller for tracking the position of the linear motor.
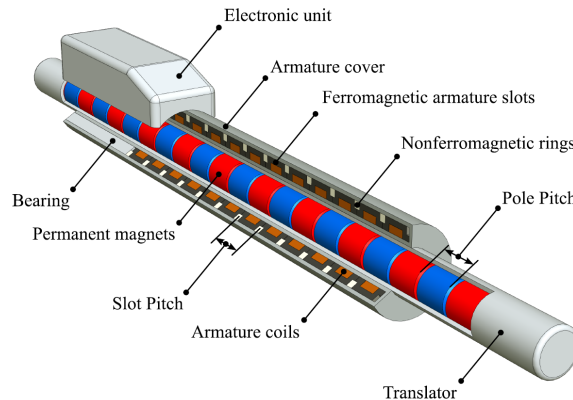

Figure 1. Structure of tubular linear motor

In recent years, sensorless control for linear permanent magnet motor have received a great deal of attention from industrial applications including: linear tubular motors [12], [18], [19], position sensorless control [4], [20], [21], end-effects [11], [22], [23]. Most of the researches on sensorless approach for linear permanent magnet motors has taken advantage of back electromotive (EMF) [19], [24], currents, and voltages into account to observe the velocity. Unfortunately, the main drawbacks of these methods are that the measurement of currents and voltage usually contain unexpected noise due to the impact of a power converter [25]. Moreover, at low speed or stopping operation, the value of EMF could be unreliable or vanish, which leads to the difficult implementation of the sensorless approach. Further, the occurrence of uncertainty in parameters (inductance and resistance) of the TLSM may result in noticeable estimation errors. Besides, to compensate impacts on control performance of the uncertainties and modeling imprecision (e.g. friction, parameter variation, and load disturbance), the adaptive method [26], [27] is employed to determine the required thrust force. The studies however have not been concerned with the sensorless control problem. It is worth noting that the position sensor is usually mounted on TLSM and the ordinary control scheme of TLSM is illustrated by Figure 2. However, obtaining velocity from the position by taking a derivative can lead to inaccurate results due to the noise contained in a position measurement.

From the issues pointed out above, this paper concerns tracking control problems of TLSM subjected to unknown loads. By employing a novel observer-based control approach, our work aims to solve a practical problem that the velocity of TLSM can not be measured directly and differential calculation from the measured position is inaccurate. To outline, our contributions can be highlighted:

- As mentioned above, the use of sensorless approach involves difficulties in dealing with noise measurements and electrical parametric uncertainties. To alleviate these concerns, this paper provides a novel observer which requires the measured position to estimate the velocity of TLSM. This observer ensures that the velocity error exponentially converge to zero. Moreover, the method of choosing proper parameters for the observer is presented.

- In addition, the multiple-loop control design which includes both a position-velocity controller and a current controller is provided to improve performance of the tracking control problem. By using the Lyapunov direct method, the position the position and velocity tracking errors are ensured to converge to small arbitrary values.

The organization of this paper includes 5 parts as follows. The next presents a dynamic model of the TLSM in $d-q$ axis and shows the main problems in sensorless control of TLSM. In section 3, a unique velocity

observer is introduced, and asymptotic convergence of observer errors are proofed. After that, in section 4 the position-velocity tracking control system for TLSM is proposed. Later, the verification of whole system is demonstrated by simulation results in section 5. Finally, conclusions are summed up in section 6.
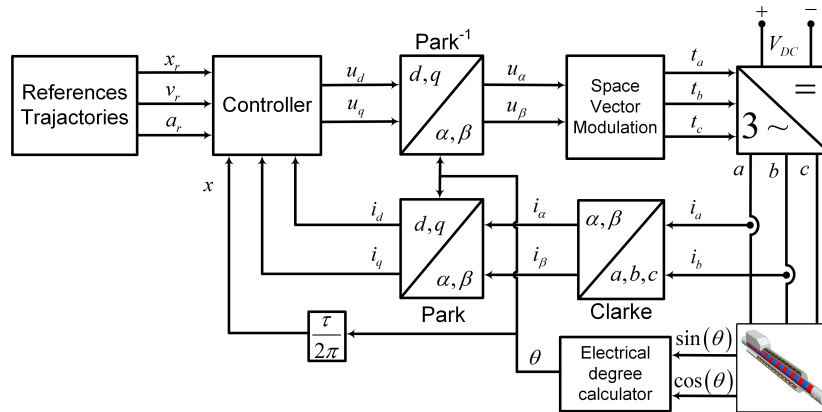

Figure 2. Typical field-oriented control (FOC) diagram of TLSM

2. PROBLEM STATEMENT

As aforementioned, the TLSM has three separated wingdings a, b, c which contain three AC currents as:

$$i_a(t) = I \sin(\omega t), \ i_b(t) = I \sin\left(\omega t + \frac{\pi}{3}\right), \ i_c(t) = I \sin\left(\omega t + \frac{2\pi}{3}\right),$$

where ω is electrical velocity of the motor. Notice that the electrical angular position of TLSM can be expressed with respect to primary position as (1)

$$\theta(t) = \frac{\pi}{\tau}x(t), \ \omega(t) = \frac{\pi}{\tau}v(t). \tag{1}$$

By using Clarke and Park transform combine with (1), the dynamic model of tubular linear motor is expressed in $d - q$ as (2)-(5):

$$\frac{dx}{dt} = v(t), \tag{2}$$

$$\frac{dv}{dt} = \frac{3\pi\psi_p}{m\tau}i_q(t) - \frac{1}{m}f_\ell(t) - \frac{1}{m}f_m(t), \tag{3}$$

$$\frac{di_d}{dt} = -\frac{R_s}{L}i_d(t) + \left(\frac{2\pi}{\tau}v(t)\right)i_q(t) + \frac{1}{L}u_d(t), \tag{4}$$

$$\frac{di_q}{dt} = -\frac{R_s}{L}i_q(t) - \left(\frac{2\pi}{\tau}v(t)\right)i_d(t) - \left(\frac{2\pi}{\tau}v(t)\right)\frac{\psi_p}{L} + \frac{1}{L}u_q(t), \tag{5}$$

where $i_d(t), i_q(t)$ are the stator current projected in d, q axis; the linear velocity and position of rotor is denoted as $v(t), x(t)$; ψ_p is the flux of the permanent magnet; R_s, L stand for, respectively, stator's resistance and inductance; m, τ represent for the slider's mass and pole step length. The inputs voltage of system in $d - q$ axis are denoted as $u_d(t)$ and $u_q(t)$. The disturbance consists two factor, the first one is the disturbance load $f_\ell(t)$, the other one is the force generate by inductance fluctuation [24] combines with the detent force [28] which is represented as $f_m(t)$.

To be specific, the reference position and velocity of the TLSM are denoted as $x_r(t), v_r(t)$. The goal of this research is to control both position and velocity of the TLSM, by which the actual position and velocity follow the desired trajectory, $x_r(t)$ and $v_r(t)$, with desired small errors and robust against the load variations. In fact, rotation motors can be easily setup velocity measurements by attaching a encoder or resolver, that of

linear motors however is challenging due to mount, high cost and sensitive with external factor like humidity, temperature, vibration. To alleviate these concerns, a novel observer is designed to estimate the velocity from available data of the position and current sensor. In addition to concern reluctance effects and force ripple reduction, $i_d(t)$ should be regulated to the reference $i_{dr}(t) = 0$.

3. VELOCITY OBSERVER DESIGN

Shortly, let us define $f_d(t)$ as the sum of disturbance i.e $f_d(t) = \frac{1}{m}f_\ell(t) + \frac{1}{m}f_m(t)$. Furthermore, the disturbance is assumed to be bounded such that

$$|f_d(t)| \leq F_m, \ |\dot{f_d}(t)| \leq dF_m, \tag{6}$$

where F_m and dF_m are given positive constants. The following observer plays a key role in the derivation of our approach

$$\begin{cases} \dot{\hat{x}}(t) = \hat{v}(t) + \rho_x\big(x(t) - \hat{x}(t)\big), \\ \dot{\hat{v}}(t) = \frac{3\pi\psi_p}{m\tau}i_q(t) + \rho_v\big(x(t) - \hat{x}(t)\big) + \gamma\text{sign}\big(x(t) - \hat{x}(t)\big), \end{cases} \tag{7}$$

in which ρ_x, ρ_v, γ are real positive constants, and $\hat{x}(0) = x(0)$. Let $\widetilde{x}(t) = x(t) - \hat{x}(t)$, $\widetilde{v}(t) = v(t) - \hat{v}(t)$, then the observer errors dynamics can be obtained by the help of (2), (3) and (7) as (8)

$$\begin{cases} \dot{\widetilde{x}}(t) = -\rho_x\widetilde{x}(t) + \widetilde{v}(t), \\ \dot{\widetilde{v}}(t) = -\rho_v\widetilde{x}(t) - \gamma\text{sign}\big(\widetilde{x}(t)\big) - f_d(t). \end{cases} \tag{8}$$

The following theorem provides a choice of observer parameters ρ_x, ρ_v, γ by which the observer (8) are well-posed.

Theorem 1: For proper positive constants $\alpha > 0$, let ρ_x, ρ_v, γ satisfying

$$\begin{bmatrix} \rho_x\rho_v & 0 \\ 0 & \rho_x \end{bmatrix} \geq 2\alpha \begin{bmatrix} \rho_v + \frac{1}{2}\rho_x^2 & \frac{1}{2}\rho_x \\ \frac{1}{2}\rho_x & 1 \end{bmatrix}, \tag{9}$$

$$\frac{\gamma\rho_x}{2} - \frac{\rho_x F_m}{2} - dF_m \geq 2\alpha(\gamma + F_m), \tag{10}$$

the system (8) is exponentially stable. Moreover, there exist $c_1, c_2 > 0$ such that

$$|\widetilde{x}(t)| < c_1 e^{-\alpha t}, \ |-\rho_x\widetilde{x}(t) + \widetilde{v}(t)| < c_2 e^{-\alpha t}.$$

Proof of Theorem 1: Denoting $\zeta_1(t) = \widetilde{x}(t)$, $\zeta_2(t) = -\rho_x\widetilde{x}(t) + \widetilde{v}(t)$ and $\zeta(t) = [\zeta_1(t), \zeta_2(t)]^T$, then (8) can be rewritten as (11)

$$\dot{\zeta}_1(t) = \zeta_2(t),$$
$$\dot{\zeta}_2(t) = -\rho_x\dot{\widetilde{x}}(t) + \dot{\widetilde{v}}(t) \tag{11}$$
$$= -\rho_x\zeta_2(t) - \rho_v\zeta_1(t) - \gamma\text{sign}\big(\zeta_1(t)\big) - f_d(t).$$

Examine the function as (12)

$$V_1(t, \zeta(t)) = \frac{1}{2}\zeta_2^2(t) + \left(\frac{\rho_v}{2} + \frac{\rho_x^2}{4}\right)\zeta_1^2(t) + \gamma|\zeta_1(t)| + f_d(t)\zeta_1(t) + \frac{\rho_x}{2}\zeta_1(t)\zeta_2(t). \tag{12}$$

And recalling that $\gamma > F_m$, we have $\gamma|\zeta_1(t)| > \big|f_d(t)\zeta_1(t)\big|$. Then, $V_1(t, \zeta(t))$ is a positive real function, furthermore it has $V_1(t, 0) = 0$, $V_1(t, \zeta(t)) > 0 \ \forall\zeta(t) \neq 0$, and $V_1(t, \zeta(t)) \to \infty$ as $||\zeta(t)|| \to \infty$. According to solution of (11), let us take the time derivative of (12) as (13)

$$\dot{V}_1(t, \zeta(t)) = \zeta_2(t)\dot{\zeta}_2(t) + \left(\rho_v + \frac{\rho_x^2}{2}\right)\zeta_1(t)\zeta_2(t) + \gamma\zeta_2(t)\text{sign}\big(\zeta_1(t)\big) + f_d(t)\zeta_2(t)$$

$$+ \dot{f_d}(t)\zeta_1(t) + \frac{\rho_x}{2}\zeta_2^2(t) + \frac{\rho_x}{2}\zeta_1(t)\dot{\zeta}_2(t)$$

$$= -\frac{\rho_x}{2}\zeta_2^2(t) + \dot{f_d}(t)\zeta_1(t) + \frac{\rho_x}{2}\zeta_1(t)\big(-\rho_v\zeta_1(t) - \gamma\text{sign}\big(\zeta_1(t)\big) - f_d(t)\big)$$

$$= -\frac{\rho_x}{2}\zeta_2^2(t) - \frac{\rho_x\rho_v}{2}\zeta_1^2(t) + \zeta_1(t)\left(-\frac{\gamma\rho_x}{2}\text{sign}\big(\zeta_1(t)\big) - \frac{\rho_x}{2}f_d(t) + \dot{f_d}(t)\right). \tag{13}$$

Using γ in theorem 1, it is worth mentioning that

$$\frac{\gamma \rho_x}{2} > \left| -\frac{\rho_x}{2} f_d(t) + \dot{f}_d(t) \right|. \tag{14}$$

In the light of (14), (13) results in

$$\dot{V}_1(t, \zeta(t)) \leq -\frac{\rho_x}{2} \zeta_2^2(t) - \frac{\rho_x \rho_v}{2} \zeta_1^2(t) - \left(\frac{\gamma \rho_x}{2} - \frac{\rho_x F_m}{2} - dF_m \right) |\zeta_1(t)|. \tag{15}$$

From (10), (15) is ensured by

$$V_1(t, \zeta(t)) \leq \frac{1}{2} \zeta^T(t) \begin{bmatrix} \rho_v + \frac{1}{2} \rho_x^2 & \frac{1}{2} \rho_x \\ \frac{1}{2} \rho_x & 1 \end{bmatrix} \zeta(t) + (\gamma + F_m) |\zeta_1(t)|.$$

By recalling conditions (9) and (10), it leads to $\dot{V}_1(t, \zeta(t)) \leq -2\alpha V_1(t, \zeta(t))$. Then, using comparison lemma in Lemma 3.4 [29] and the initial condition $\widetilde{x}(0) = \zeta_1(0) = 0$, we have that

$$V_1(t, \zeta(t)) \leq V_1(0, \zeta(0)) e^{-2\alpha t} = \frac{1}{2} \widetilde{v}^2(0) e^{-2\alpha t}.$$

Accordingly, $\zeta_1(t)$ and $\zeta_2(t)$ exponentially converge. Then, exist $c_1, c_2 > 0$ such that $\zeta_1^2(t) < c_1^2 V_1(t, \zeta(t))$, $\zeta_2^2(t) < c_2^2 V_1(t, \zeta(t))$. Obviously, the theorem 1 is proved.

Remark 1: With the assumption of no load disturbance ($f_d(t) \equiv 0$), the switching term in (7) is no longer needed. By excluding the switching term, the proposed observer be become the high-gain observer as in [30]. Hence, the observer (7) can be seen as an improvement for high-gain observer that address to handle the impact of disturbance.

4. CONTROLLER DESIGN

Using a cascade control strategy, we separate the TLSM system as presented in (2)-(5) into two subsystems which are position-velocity (outer subsystem) and current subsystem (inner subsystem). It should be noted that the time response of inner subsystem is much faster than that of the outer subsystem. The two control loops are present as follows.

4.1. Velocity-position controller

For simplicity sake, The desired velocity and acceleration is respectively denoted as $v_r(t) = \dot{x}_r(t)$, $a_r(t) = \dot{v}_r(t)$. Further, we define these following symbols

$$\sigma = \frac{3\pi\psi}{m\tau}, \; e_x(t) = x(t) - x_r(t), \tag{16}$$
$$e_v(t) = v(t) - v_r(t), \; \hat{e}_v(t) = \hat{v}(t) - v_r(t),$$

And follow the position-velocity subsystem in (2)-(3) becomes

$$\begin{aligned} \dot{e}_x(t) &= e_v(t), \\ \dot{e}_v(t) &= \sigma i_q^* - a_r(t) - f_d(t), \end{aligned} \tag{17}$$

In which i_q^* stands for the reference quadrature current which is assigned to inner control loop. Apply the assumption that $i_q(t)$ simultaneously track i_q^*. Then, replaced i_q with $i_q^*(t)$ in (17). The controller for outer loop is provided as (18)

Theorem 2: Consider

$$i_q^* = \frac{1}{\sigma} \big(a_r(t) - k_x e_x(t) - k_v \hat{e}_v(t) \big), \tag{18}$$

If $k_x, k_v \in \mathbb{R}_{++}$ are large enough constants, then, the outer loop (17) is stable, and $e_x(t), e_v(t)$ converge to arbitrary small values.

Proof of Theorem 2: Using notations in (16), it lead to $\hat{e}_v(t) = e_v(t) - \widetilde{v}(t)$. Then, (17) can be rewritten as (19)

$$
\begin{aligned}
\dot{e}_x(t) &= e_v(t), \\
\dot{e}_v(t) &= -k_x e_x(t) - k_v e_v(t) + k_v \widetilde{v}(t) - f_d(t).
\end{aligned}
\tag{19}
$$

On studying the control performance and stability of the closed loop system, a Lyapunov candidate function is applied as

$$
V_2(t) = \frac{1}{2}(k_x + k_v)e_x^2(t) + \frac{1}{2}e_v^2(t) + e_x(t)e_v(t) + \dot{V}_1(t).
$$

By using (19), it establishes that

$$
\begin{aligned}
\dot{V}_2(t) =& (k_x + k_v)e_x(t)e_v(t) + e_v(t)\dot{e}_v(t) + e_v^2(t) + e_x(t)\dot{e}_v(t) + \dot{V}_1(t) \\
=& -k_x e_x^2(t) - (k_v - 1)e_v^2(t) + k_v \widetilde{v}(t)\big(e_x(t) + e_v(t)\big) - f_d(t)\big(e_x(t) + e_v(t)\big) + \dot{V}_1(t).
\end{aligned}
\tag{20}
$$

From (15), it is clear that $\dot{V}_1(t) \leq -\frac{\rho_x}{8}(\rho_x \zeta_1(t) + \zeta_2(t))^2 = \frac{\rho_x}{8}\widetilde{v}^2(t)$. By applying the inequalities as

$$
\big|\widetilde{v}(t)\big(e_x(t) + e_{iq}(t)\big)\big| \leq \epsilon_x e_x^2(t) + \epsilon_v e_v^2(t) + \left(\frac{1}{4\epsilon_x} + \frac{1}{4\epsilon_v}\right)\widetilde{v}^2(t),
$$

$$
\big|f_d(t)\big(e_x(t) + e_v(t)\big)\big| \leq \frac{F_m^2}{2\epsilon_f} + \epsilon_f\big(e_x^2(t) + e_v^2(t)\big),
$$

where $\epsilon_x, \epsilon_v, \epsilon_f > 0$, from (20) we obtain that

$$
\begin{aligned}
\dot{V}_2(t) \leq& -(k_x - \epsilon_x - \epsilon_f)e_x^2(t) - (k_v - \epsilon_v - \epsilon_f - 1)e_v^2(t) \\
& -\left(\frac{\rho_x}{8} - \frac{1}{4\epsilon_x} - \frac{1}{4\epsilon_v}\right)\widetilde{v}^2(t) + \frac{F_m^2}{2\epsilon_f}.
\end{aligned}
\tag{21}
$$

Accordingly, by choosing

$$
\begin{aligned}
k_x - \epsilon_x - \epsilon_f &= 1, \\
k_v - \epsilon_v - \epsilon_f - 1 &= 1, \\
2\rho_x - \epsilon_x^{-1} - \epsilon_v^{-1} &> 0.
\end{aligned}
\tag{22}
$$

Then $\dot{V}_2(t) < 0$ for all $\big(e_v(t), e_x(t)\big) \notin \mathcal{E}$ where

$$
\mathcal{E} \triangleq \left\{(e_x, e_v) \in \mathbb{R}^2 : e_x^2 + e_v^2 \leq \frac{F_m^2}{2\epsilon_f}\right\}.
\tag{23}
$$

It implies that the tracking errors $(e_v(t), e_x(t))$ enter $\mathcal{E}$ in finite time due to $\dot{V}_2(t) < 0$. By choosing ϵ_f large enough, the tracking errors can converges to arbitrary small values. Intuitively, the theorem 2 is proved.

4.2. Current controller

From the fact that dynamics of the current loop is always much faster than that of outer loop, the reference i_q^* can be assumed to be unvarying in inner-loop control process. Additionally, the inconstancy in inductance cause by end-effect phenomenon can be neglected. Continuously, the following notations are provided

$$
e_{iq}(t) = i_q(t) - i_q^*, \ e_{id}(t) = i_d(t) - i_d^*.
$$

In what follows, let us establish a modified PI controller which cooperates with the velocity observer in section 3. The current loop can be consider as two parallel current system and therefore can be controlled by two PI-like controller as (24), (25)

$$
u_d(t) = R_s i_d^* - k_d e_{id}(t) - k_{id}\int_0^t e_{id}(\xi)d\xi - \frac{2\pi L}{\tau}i_q(t)\hat{v}(t),
\tag{24}
$$

$$
u_q(t) = R_s i_q^* - k_q e_{iq}(t) - k_{iq}\int_0^t e_{iq}(\xi)d\xi + \left(\frac{2\pi L}{\tau}i_d(t) + \frac{2\pi \psi_p}{\tau}\right)\hat{v}(t).
\tag{25}
$$

In which k_d, K_p, k_{id}, k_{iq} are positive constants. From that, the inner closed-loop is derived

$$\dot{e}_{id}(t) = -\frac{k_d + R_s}{L}e_{id}(t) - \frac{k_{id}}{L}\int_0^t e_{id}(\xi)d\xi + \frac{2\pi}{\tau}i_q(t)\tilde{v}(t), \tag{26}$$

$$\dot{e}_{iq}(t) = -\frac{k_q + R_s}{L}e_{iq}(t) - \frac{k_{iq}}{L}\int_0^t e_{iq}(\xi)d\xi - \left(\frac{2\pi}{\tau}i_d(t) + \frac{2\pi\psi_p}{\tau L}\right)\tilde{v}(t). \tag{27}$$

Using the same method which presented in subsection 4.1, by applying the Lyapunov candidate function as in (28)

$$V_I(t) = V_1(t) + \frac{1}{2}e_{id}^2(t) + \frac{1}{2}e_{iq}^2(t) + \frac{k_{id}}{2L}\left(\int_0^t e_{id}(\xi)d\xi\right)^2 + \frac{k_{iq}}{2L}\left(\int_0^t e_{iq}(\xi)d\xi\right)^2. \tag{28}$$

It is clear that the tracking errors of both quadrature and direct current converge to zero. In concluded, the control scheme whole system is describe in Figure 3.
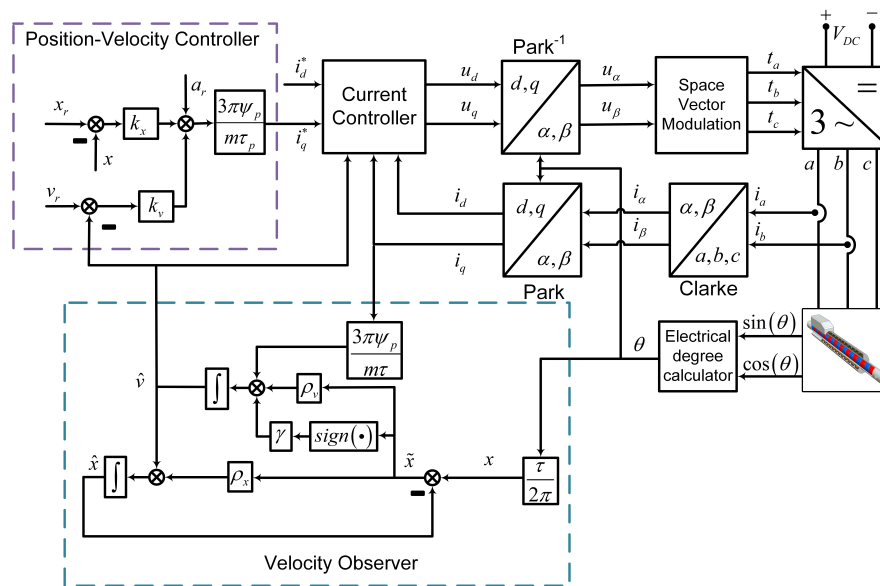
Figure 3. The proposed control diagram for the TLSM

5. SIMULATION RESULT AND ANALYSIS

TLSM is used in this simulation has the parameters as follow: $R_s = 10.3 (Ohm); m = 0.171 (kg);$ $L = 1.4 (mH); n_p = 1; \tau = 10 (mm); \psi_p = 0.035 (Wb)$. This motor is mounted a position sensor in which output data are $sin(\theta)$ and $cos(\theta)$. The control performances of the sensorless approach are verified by two difference simulation scenarios. On one hand, the first scenario verifies the effectiveness of the control system in the case of no measurement noise affect the TLSM. In the other hand, the other test is done with the impact of measurement noise to the position feedback signal. In both scenarios, the using controller, observer and disturbance load are the same.

The simulation of the observer based control for TLSM is ran on MATLAB/Simulink with the chosen sampling time is $10^{-5}(s)$. The load's disturbance applied to TLSM given by: $f_\ell(t) = 3 + \frac{16}{\pi}\sin(20t) + \frac{16}{3\pi}\sin(60t) + \frac{16}{5\pi}\sin(100t)$. It is worth mentioning that, in practical case, $f_m(t)$ is very small in compare with $f_\ell(t)$. Therefore, we take $F_m = 60, dF_m = 2000$. From (9), (10), observer's parameters (7) are given by $\rho_x = 10^3, \rho_v = 2.10^4, \gamma = 100, \alpha = 30$. Following (22), the parameters of controller block are chosen as $K_p = 10^5, k_v = 2.10^3, k_d = K_p = 10, k_{id} = k_{iq} = 10^4$.

5.1. None measurement noise case

As mention above, the feedback position from sensor is assumed perfectly accurate, the initial errors of observed position and velocity are chosen as $\tilde{x}(0) = 0, \tilde{v}(0) = 0.1$. As illustrated in Figures 4(a) and 4(b),

the actual position and actual velocity of TLSM follow the desired trajectories. Also, there are variations in tracking errors in Figures 4(c) and 4(d) during the response period of the observer. Values of the current and voltage of the q-axis are shown in Figures 5(a) and 5(b). Although the error still converges to zero in less than 0.1 s Figure 5(c), the TLSM is affected by the disturbance load as in Figure 5(d). During this interval, the motor stay still, which is the advantage of propose velocity observer compare with the other EMF-based techniques. Accordingly, theorem 1 is verified. Furthermore, under the disturbance load, the position tracking is still maintained. Figure 5(a) depicts that the actual quadrature current $i_q(t)$ follows the desired signal i_q^*. With the high precision tracking and quick response time, the simulated results confirm the preformance of the propose control system for TLSM.
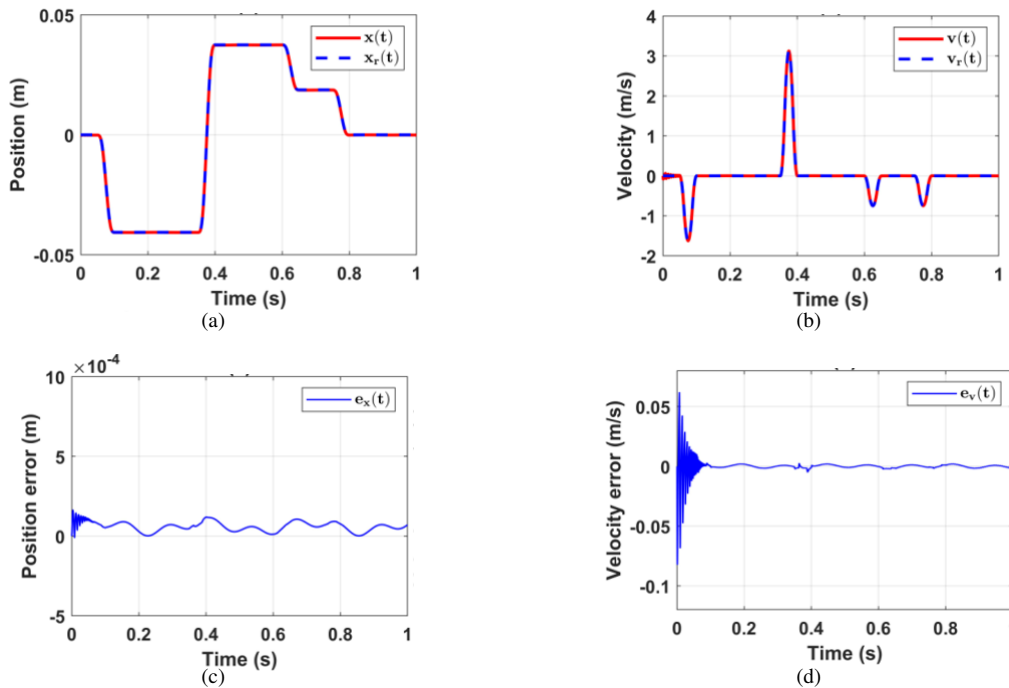
Figure 4. Position and velocity behavior of the TLSM, (a) position, (b) velocity (c) position error, and (d) velocity error

5.2. Presence of measurement noise case

In this case, opposition from the first case, The data from position sensor is assumed to contain measurement noise as (29)

$$x_{meas}(t) = x(t) + n(t), \tag{29}$$

in which $x_{meas}(t)$ denotes the measured signal from the position sensor, and $n(t)$ is a noise measurement which is normally modelled by a white process. Difference from the first case, the initial error of observed position is not equal to zero due to the measurement noise. Therefore, the initial errors of observed position and velocity are chosen as $\tilde{x}(0) = 5.10^{-3}$, $\tilde{v}(0) = 0.1$. With the measurement signal as depicted in Figure 6(a), the widely used method which consist low-pass filter combine with derivatives can not obtain the accurate velocity. The voltage value is illustrated in Figure 6(b). Overall, the proposed controller still outweigh in position tracking control, as depicted in Figures 6(c) and 6(d). Current and velocity values are shown in Figures 7(a) and 7(b). As illustrated in Figures 7(c) and 7(d), the errors between actual and observed values converge in approximately 0.1 s and no greater than 0.05 (m/s) with velocity and 0.002 (m) with position errors.
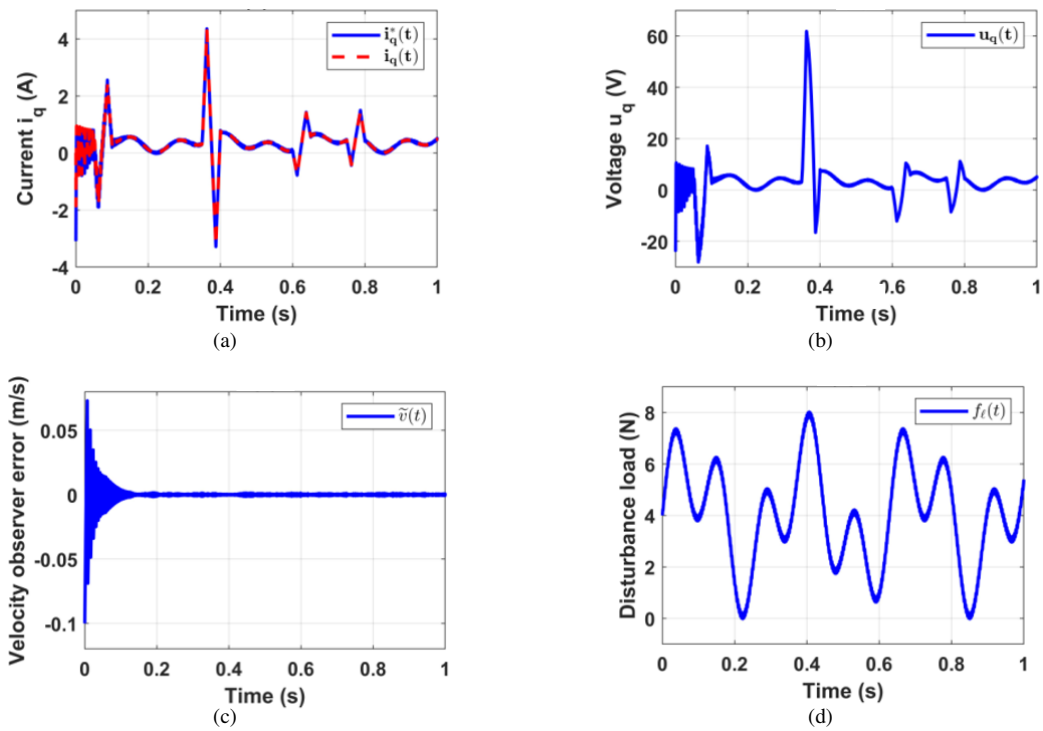
Figure 5. Time response of the TLSM without measurement noise, (a) current i_q, (b) voltage u_q, (c) velocity observer error, and (d) disturbance load
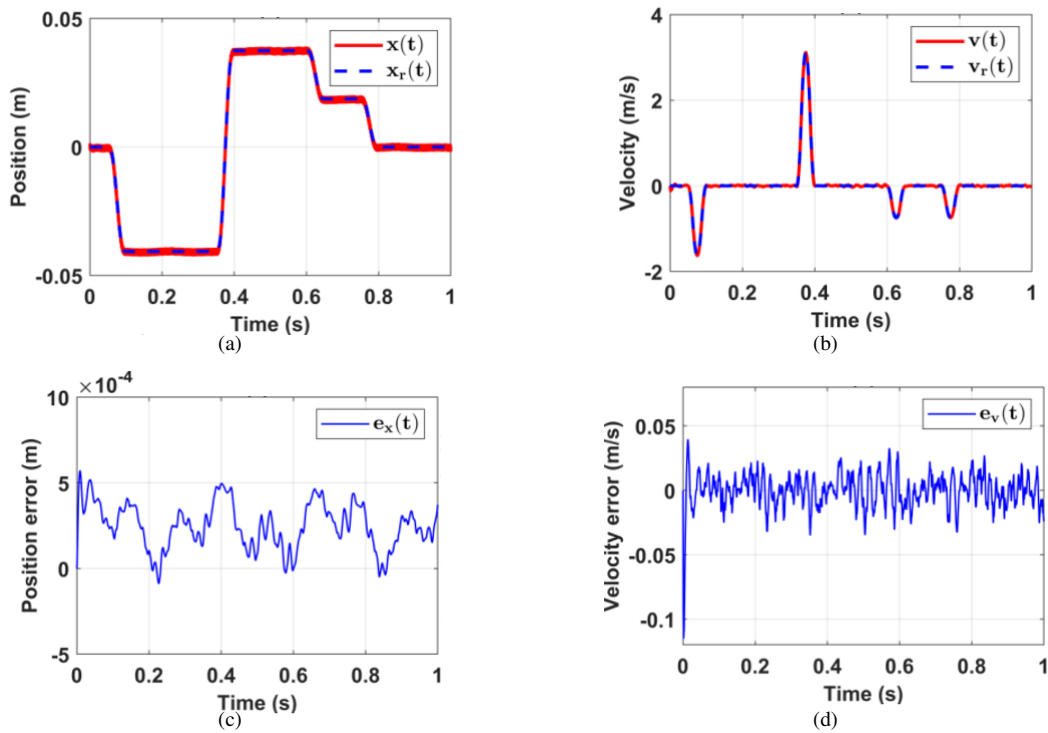

Figure 6. Position and velocity behavior of the TLSM under noise measurement, (a) position, (b) velocity, (c) position error, and (d) velocity error
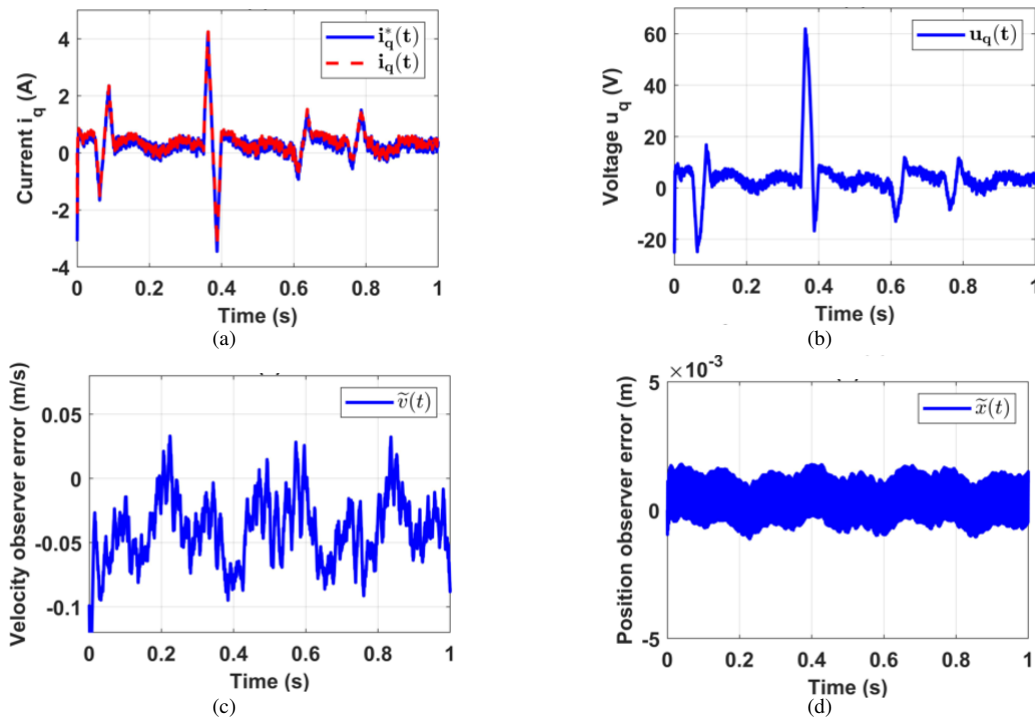
Figure 7. Time response of the TLSM under measurement noise, (a) current i_q, (b) voltage u_q, (c) velocity observer error, and (d) position observer error

Remark 2: Under the impact of measurement noise $n(t)$, the traditional method [31] which obtain the velocity via a differential calculation of measured position can not estimate the actual velocity. It should be noted that employing low-pass filters on measured signal seems to be ineffective because the measurement noise often is not considered a deterministic signal. Additionally, the use of Kalman filter [32], [33] in this case possibly results in the large velocity estimation error due to the effects of unknown disturbance load in velocity dynamics. Further, at low speed or stopping operation, the value of EMF could be unreliable or vanish, the EMF approach [19], [24] leads to the difficult and inaccurate velocity estimation. From the above analyses of previous approaches, the proposed method shows advantages in the velocity estimation in the occurrence of measurement noise $n(t)$.

6. CONCLUSION

This note has provided a novel technical solution for the sensorless tracking control problem of TLSM under the lack of velocity sensors and unknown disturbance loads. The main contributions of our method have based on the proposed velocity-observer, which ensures asymptotic the convergence of observer errors. By cooperating with the observer, the position-velocity tracking controller and current controllers have been constructed by using Lyapunov direct method. These controllers have ensured that the position and velocity error converges to arbitrarily small values by choosing properly control parameters. In later work, the current sensorless control will be taken into account with no further sensor requirement in control TLSM.

REFERENCES

[1]   J. F. Gieras, Z. J. Piech, and B. Tomczuk, *Linear synchronous motors: transportation and automation systems.* CRC press, 2018.

[2]   I. Boldea, *Linear electric machines, drives, and MAGLEVs handbook.* CRC press, 2017.
[3]   D. Naso, F. Cupertino, and B. Turchiano, "Precise position control of tubular linear motors with neural networks and composite learning," *Control Engineering Practice,* vol. 18, no. 5, pp. 515–522, 2010.
[4]   J. Wang, W. Wang, and K. Atallah, "Kalman filter based sensorless control of a tubular permanent magnet machine for active vehicle suspension," 5th IET International Conference on Power Electronics, Machines and Drives (PEMD 2010), 2010, doi: https://doi.org/10.1049/cp.2010.0072.
[5]   A. Maruo, H. Igarashi, H. Oshima, and S. Shimokawa, "Optimization of planar magnet array using digital annealer," *IEEE Transactions on Magnetics,* vol. 56, no. 3, pp. 1-4, 2020, doi: 10.1109/TMAG.2019.2957805.
[6]   M.-S. Tran and S.-J. Hwang, "Design and experiment of a moving magnet actuator based jetting dispenser," *Applied Sciences,* vol. 9, no. 14, 2019.
[7]   D. Pérez, L. Candela, M. Torralba Gracia, J. A. Albajez Garc´ıa, and J. A. Yagüe Fabra, "One-dimensional control system for a linear motor of a two-dimensional nanopositioning stage using commercial control hardware," *Micromachines,* vol. 9, no. 9, 2018.
[8]   T. Ji, X. Huang, and W. Zhou, "Thrust optimization of double primary tubular linear synchronous motor based on neural network surrogate model," in *2019 22nd International Conference on Electrical Machines and Systems (ICEMS),* 2019, pp. 1–6.
[9]   N. H. Quang, N. P. Quang, N. N. Hien, and N. T. Binh, "Min max model predictive control for polysolenoid linear motor," *International Journal of Power Electronics and Drive Systems (IJPEDS),* vol. 9, no. 4, pp. 1667-1675, 2018, doi: 10.11591/ijpeds.v9i4.pp1666-1675.
[10]   H. Q. Nguyen, P. Q. Nguyen, D. P. Nam, and T. B. Nguyen, "Multi parametric model predictive control based on laguerre model for permanent magnet linear synchronous motors," *International Journal of Electrical and Computer Engineering (IJECE),* vol. 9, no. 2, pp. 1067-1077, 2019, doi: 10.11591/ijece.v9i2.pp1067-1077.
[11]   D. Xu, J. Huang, X. Su, and P. Shi, "Adaptive command-filtered fuzzy backstepping control for linear induction motor with unknown end effect," *Information Sciences,* vol. 477, pp. 118–131, 2019.
[12]   M. K. Bani Melhem, M. Simic, C. Y. Lai, Y. Feng, and S. Ding, "Fuzzy control of the dual-stage feeding system consisting of a piezoelectric actuator and a linear motor for electrical discharge machining," *Proceedings of the Institution of Mechanical Engineers, Part B: Journal of Engineering Manufacture,* vol. 234, no. 5, 2020, pp. 945–955.
[13]   N. Shieh, P. Tung, and C. Lin, "Robust output tracking control of a linear brushless DC motor with time-varying disturbances," *IEE Proceedings-Electric Power Applications,* vol. 149, no. 1, pp. 39–45, 2002, doi: 10.1049/ip-epa:20020027.
[14]   H.-j. Song, L. Liu, M.-j. Cai, and N. Shao, "Backstepping sliding mode control for the displacement tracking of permanent magnet linear synchronous motor based on nonlinear disturbance observer," in *Proceedings of the 11th International Conference on Modelling, Identification and Control (ICMIC2019),* 2020, pp. 373–382, doi: 10.1007/978-981-15-0474-7_35.
[15]   S. Nagai, T. Nozaki, and A. Kawamura, "Real-time sensorless estimation of position and force for solenoid actuators," *IEEJ Journal of Industry Applications,* vol. 5, no. 2, pp. 32–38, 2016.
[16]   P. Sun, "Adaptive robust motion control of an ironless permanent magnet linear synchronous motor with dead-zone compensation," in *2019 22nd International Conference on Electrical Machines and Systems (ICEMS),* 2019, pp. 1–5, doi: 10.1109/ICEMS.2019.8921888.
[17]   Z. Wang, C. Hu, Y. Zhu, S. He, K. Yang, and M. Zhang, "Neural network learning adaptive robust control of an industrial linear motor-driven stage with disturbance rejection ability," *IEEE Transactions on Industrial Informatics,* vol. 13, no. 5, pp. 2172–2183, 2017, doi: 10.1109/TII.2017.2684820.
[18]   F. Cupertino, P. Giangrande, G. Pellegrino, and L. Salvatore, "End effects in linear tubular motors and compensated position sensorless control based on pulsating voltage injection," *IEEE Transactions on Industrial Electronics,* vol. 58, no. 2, pp. 494–502, 2010, doi: 10.1109/TIE.2010.2046577.
[19]   H. A. Hussain and H. A. Toliyat, "Back-EMF based sensorless vector control of tubular PM linear motors," in *2015 IEEE International Electric Machines & Drives Conference (IEMDC),* 2015, pp. 878–883.
[20]   P.-Q. Yu, Y.-H. Lu, Y. Wang, W.-M. Yang, and Z.-C. Chen, "Research on permanent magnet linear synchronous motor position sensorless control system," in *Zhongguo Dianji Gongcheng Xuebao (Proceedings of the Chinese Society of Electrical Engineering),* vol. 27, no. 24, 2007, pp. 53–57.
[21]   F. Cupertino, G. Pellegrino, P. Giangrande, and L. Salvatore, "Sensorless position control of permanent-magnet motors with pulsating current injection and compensation of motor end effects," *IEEE Transactions on Industry Applications,* vol. 47, no. 3, pp. 1371–1379, 2011.
[22]   P. Giangrande, F. Cupertino, and G. Pellegrino, "Modelling of linear motor end-effects for saliency based sensorless control," in *2010 IEEE Energy Conversion Congress and Exposition,* 2010, pp. 3261-3268, doi: 10.1109/ECCE.2010.5618349.
[23]   A. Accetta, M. Cirrincione, M. Pucci, and G. Vitale, "Neural sensorless control of linear induction motors by a full-order luenberger observer considering the end effects," *IEEE Transactions on Industry Applications,* vol. 50, no. 3, pp. 1891–1904, 2013, doi: 10.1109/TIA.2013.2288429.

[24] W. Zhao, S. Jiao, Q. Chen, D. Xu, and J. Ji, "Sensorless control of a linear permanent-magnet motor based on an improved disturbance observer," *IEEE Transactions on Industrial Electronics*, vol. 65, no. 12, pp. 9291–9300, 2018.

[25] M. I. F. M. Hanif, M. H. Suid, and M. A. Ahmad, "A piecewise affine PI controller for buck converter generated DC motor," *International Journal of Power Electronics and Drive System (IJPEDS)*, vol. 10, no. 3, pp. 1419–1426, 2019, doi: 10.11591/ijpeds.v10i3.pp1419-1426.

[26] F.-J. Lin and P.-H. Chou, "Adaptive control of two-axis motion control system using interval type-2 fuzzy neural network," *IEEE Transactions on Industrial Electronics*, vol. 56, no. 1, pp. 178–193, 2008, doi: 10.1109/TIE.2008.927225.

[27] Y.-S. Kung, "Design and implementation of a high-performance PMLSM drives using DSP chip," *IEEE transactions on industrial electronics*, vol. 55, no. 3, pp. 1341–1351, 2008, doi: 10.1109/TIE.2007.909736.

[28] K.-C. Lim, J.-K. Woo, G.-H. Kang, J.-P. Hong, and G.-T. Kim, "Detent force minimization techniques in permanent magnet linear synchronous motors," *IEEE Transactions on Magnetics*, vol. 38, no. 2, pp. 1157–1160, 2002, doi: 10.1109/20.996296.

[29] H. K. Khalil and J. W. Grizzle, Nonlinear systems. Prentice hall Upper Saddle River, 2002.

[30] A. Atassi and H. Khalil, "Separation results for the stabilization of nonlinear systems using different high-gain observer designs," *Systems & Control Letters*, vol. 39, no. 3, pp. 183–191, 2000, doi: 10.1016/S0167-6911(99)00085-7.

[31] N. P. Quang, and J.-A. Dittrich, *Vector control of three-phase AC machines*, Springer, 2008.

[32] Y.-R. Chen, N. C. Cheung, and J. Wu, "Sensorless drive of permanent magnet linear motors using modified Kalman filter," in *2001 IEEE 32nd Annual Power Electronics Specialists Conference (IEEE Cat. No. 01CH37230)*, vol. 4, 2001, pp. 2009–2013, doi: 10.1109/PESC.2001.954416.

[33] A. Qiu, B. Wu, and H. Kojori, "Sensorless control of permanent magnet synchronous motor using extended Kalman filter," in *Canadian Conference on Electrical and Computer Engineering 2004 (IEEE Cat. No. 04CH37513)*, vol. 3, 2004, pp. 1557–1562, doi: 10.1109/CCECE.2004.1349704.

BIOGRAPHIES OF AUTHORS

Nguyen Hong Quang received a Ph.D. of control engineering and automation from Thai Nguyen University of Technology (TNUT), Vietnam, in 2019. He is currently a lecturer at the Faculty of Mechanical, Electrical, Electronics Technology. His research interests include electrical drive systems, control systems, and their applications, adaptive dynamic programming control, robust nonlinear model predictive control, motion control, and mechatronics. Email: quang.nguyenhong@tnut.edu.vn.

Nguyen Phung Quang received his Dipl.-Ing. (Uni.), Dr.-Ing. and Dr.-Ing. habil. degrees from TU Dresden, Germany in 1975, 1991 and 1994 respectively. Prior to his return to Vietnam, he had worked in Germany industry for many years, contributed to create inverters REFU 402 Vectovar, RD500 (REFU Elektronik); Simovert 6SE42, Master Drive MC (Siemens). From 1996 to 1998, he served as lecturer of TU Dresden where he was conferred as Privatdozent in 1997. He joined Hanoi University of Science and Technology in 1999, as lecturer up to now. He is currently a professor of HUST and honorary professor of TU Dresden. He was author/co-author of more than 200 journal and conference papers; 8 books with three among them was written in German and one in English entitled "Vector Control of Three-Phase AC Machines-System Development in the Practice" published by Springer in 2008, and 2nd edition in June 2015. His research interests are electrical drive systems, motion control, robotic control, vector control of electrical machines, wind and solar power systems, digital control systems, modeling and simulation. Email: quang.nguyenphung@hust.edu.vn.

Nguyen Van Lanh received the bachelor's degree in Electrical Engineering from Thai Nguyen University of Technology (TNUT), Vietnam in 2011, and Master of Control System Engineering from HAN University of Applied Science, the Netherlands in 2018. He has been working as a lecturer and researcher at the Faculty of International Training, TNUT, Vietnam since 2012. He is currently a Ph.D. student at the University of Technology Sydney, Australia. His research interests include automation, robotics, control and navigation for unmanned vehicles, and cooperative control systems. Email: vanlanh.nguyen@uts.edu.au.